

## **Numerical Investigation of Shock wave Turbulent Boundary Layer Interaction over a 2D Compression Ramp**

**Asmelash Haftu Amaha**

*Department of Aeronautical Engineering, Defence University,  
College of Engineering, Debrezeit, ETHIOPIA.*

### **Abstract**

The interaction between a shock wave and a turbulent boundary layer (SWTBLI) remains one of the most challenging problems of modern high speed fluid dynamics. The complicated nature of the interaction embodies most intriguing effects and raises difficult questions which are still largely unresolved. In the present research work, shock wave turbulent boundary layer interaction has been analyzed computationally in a two-dimensional compression ramps for a free stream Mach numbers of 2.85 and 2.94. Ramp angles ranging from 8° to 24° were used to produce the full range of possible flow fields, including flows with no separation, moderate separation, and significant amount of separation. The model has been studied based on a commercially available Computational Fluid Dynamics (CFD) Code that employs Shear Stress Transport (SST) of  $k-\omega$  turbulence model and Realizable  $k-\varepsilon$  model. The CFD code and the turbulence models used are validated by comparing with experimental results available in literature. The computed data for surface pressure distribution indicated a good comparison with the experiment. Numerical results obtained through the present series of computations indicate an increased separation and reattachment locations, when compared to experiment.

**Keywords:** high speed flows; shock wave; turbulent boundary layer; separation; turbulence models.

## 1. Introduction

A Shock wave is an exceptionally thin region that appear in nature whenever the different elements in a fluid approach one another with a velocity higher than the local speed of sound. If you imagine an aircraft travelling at supersonic speeds then you can see a shock wave around the body as shown in Fig. 1. Strong shock waves can occur: at the air-intake compression ramps of an air-breathing propulsion system, ahead of the vehicle nose, the rounded leading-edge of wings and tails, at the control surfaces, flaperon, at the rear part of an after body, etc. Shock wave boundary layer interaction is therefore a phenomena commonly associated with aerospace/aeronautical devices when a shock wave meets a boundary layer in high speed flows. Shock wave boundary layer interaction is a fact of life in the practical world of supersonic flows for both internal and external flows.

The separation of the boundary layer or its disturbance by a shock wave are two phenomena, which can involve increase in losses of total pressure, high peak heat transfer rates, hence drag and can sometimes even be catastrophic if the shock is strong enough to cause separation. The knowledge of the boundary layer which develops on the walls of these components is essential to optimize the use of these vehicles or equipments or an in-depth understanding of the phenomena is essential for efficient aerodynamic and propulsion design. [1-4]

The compression ramp interaction is a simplified case of the types of interactions that occur over deflected control surfaces. In the ramp interaction, an abrupt change in the wall inclination is the origin of a shock wave through which the incoming flow undergoes a deflection equal to the wedge angle  $\theta$ . When the ramp angle  $\theta$  is small, the overall flow structure is not much affected by the interaction taking place at the ramp origin and thus in inviscid flow, a single oblique shock at angle  $\beta$  would be generated originating from the corner location and turn the flow by an angle  $\theta$  (Fig. 2). When the ramp angle  $\theta$  is increased (hence the shock strength), the upstream influence distance (defined as the distance between the interaction onset and the ramp origin) increases accordingly the boundary layer on the flat plate experiences an adverse pressure gradient across the shock wave and separates the flow. The streamline showing the extent of separation region is plotted and the separation and reattachment points are identified by S and R. The size between S and R determines the size of the separation bubble [4].

The flow field in a compression ramp has been studied extensively by such authors as Delery (1985), Settles et al (1979), Dolling and Murphy (1983), Kuntz et al (1987), Daniel Arnal and Jean Delery (2004). Theses earlier works cover a wide range of turning angles, mach numbers and Reynolds numbers, but a clear and concrete idea of the onset of the onset of shock induced separation is still to be covered.

The first objective of the present paper is to assess the accuracy of the k- $\omega$  SST turbulence model for different ramp angles that were studied namely 8°, 16°, 20° and 24° at Mach 2.85 and 2.94. The computed flowfield results have been compared with the experimental data of references [2, 3, and 4] for surface pressure distribution. The second objective is an assessment of the separation and reattachment locations based

on surface pressure and shear stress distributions. A qualitative description of the interaction is also presented based on density contours.



Fig. 1: Shock wave on aircraft [5]

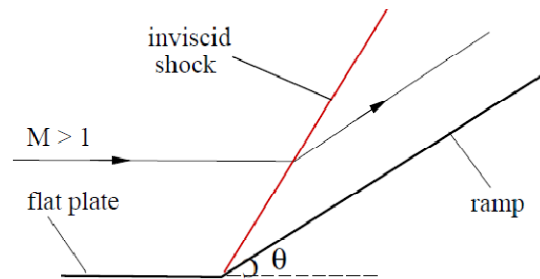
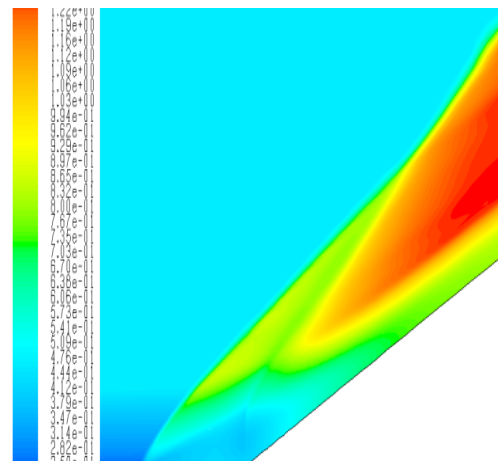
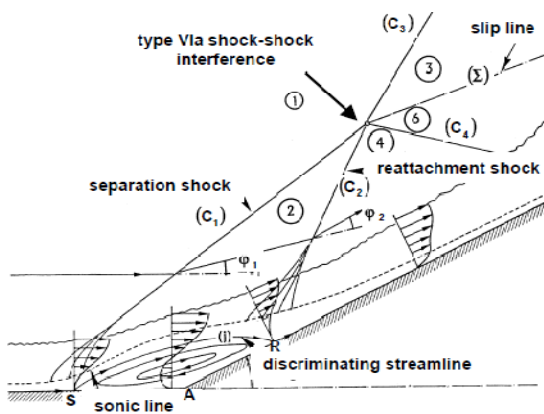


Fig. 2: Inviscid supersonic flow over compression corner generating an oblique shock at the corner.



(a) Viscous flow over compression corner with separation, reattachment shock and separated bubble [1] (b) Density contour near 24° corner flow at  $M = 2.85$

Fig. 3: Structure of ramp flow with and without boundary layer separation.

## 2. Simulation Methodology

The computational domain extends from a prescribed location upstream of the interaction where a turbulent boundary layer is generated, to a point well downstream of the interaction. Domain height is taken large enough so that shock-shock interaction does not reach that height and flow at that height is the free stream flow and is not affected by the interaction taking place near the wall. Basic mesh details of the ramp (20°) are shown in Fig. 4 with a typical grid distribution clustered near the corner region. Upstream extent used is large enough to build up the required turbulent

boundary layer thickness  $\delta = 9 \text{ mm}$ . Computations were made by using grid to grid file interpolation technique in a sequence of progressively finer grids with three different grids [Grid 1 (40000 cells), Grid 2 (80000 cells) and Grid 3 (120000 cells)] in two blocks and  $0 < y^+ < 0.35$ . Inlet conditions used are as in [4]. To simulate the different flow configurations commercially available CFD software has been used.

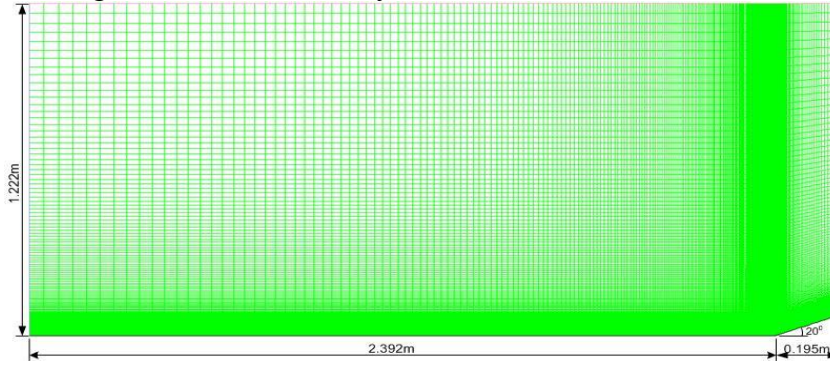
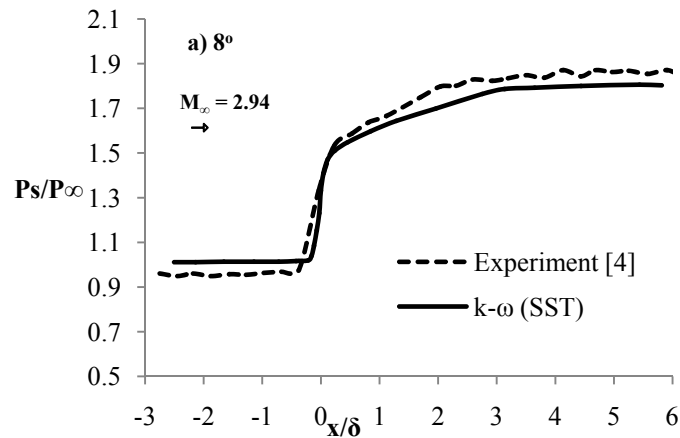


Fig. 4: Grid system (computational domain)

### 3. Results and Discussion

Comparison of computed and experimental results of the surface pressure ratio for the different ramp angles studied is shown in Fig. 5 a) to d). The pressure and x-location are non dimensionalized using the inlet static pressure of 14391 Pa and the boundary layer thickness of 9 mm, respectively. For  $8^\circ$  and  $16^\circ$  ramp flows (weak interactions) the numerical results show the same trend as the experimental results. The computations for the interaction involving the  $16^\circ$  ramp is in very good agreement with the experimental data throughout the interaction region and the variation at the location of the initial pressure rise is around 3.5%. With increasing shock strength ( $20^\circ$  and  $24^\circ$ ), the numerical results show larger upstream influence in comparison with the experimental results. This deviation from experiments is 36% and 43% in the case of the ramp angles of  $20^\circ$  and  $24^\circ$ , respectively.



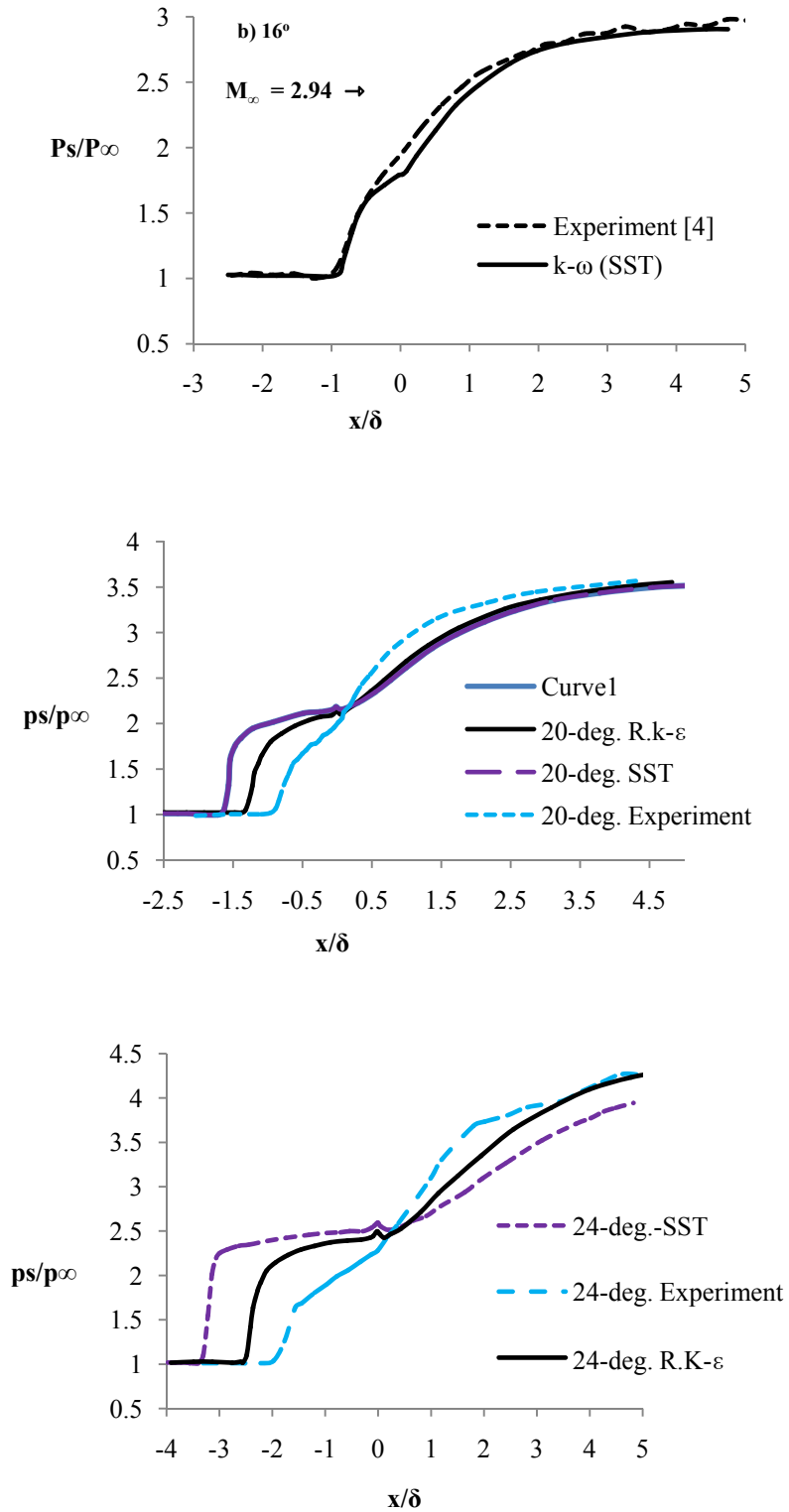
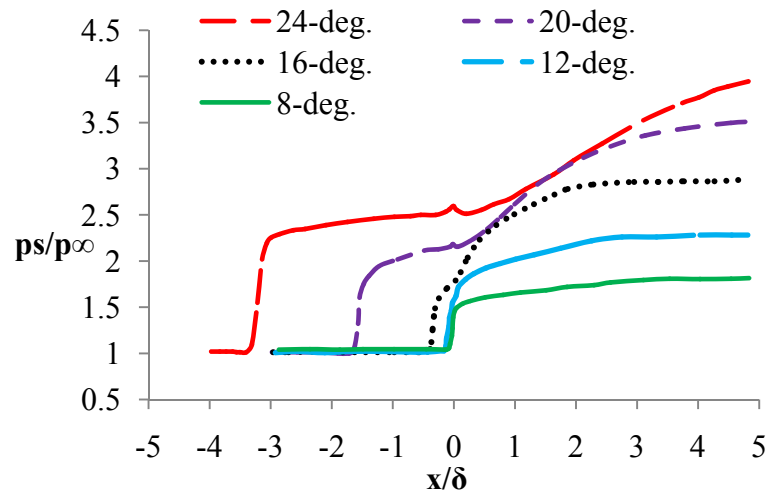
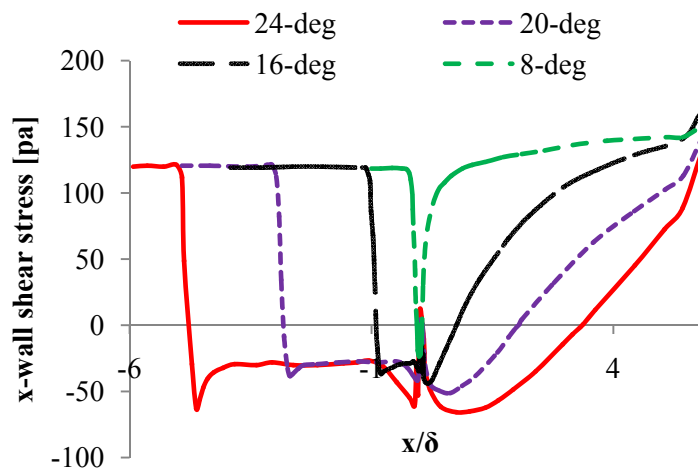


Fig. 5: Computed and experimental results for the pressure ratio.

Comparison of surface pressure distributions is shown in Fig. 6 for the ramp angles studied. The size of the plateau region increases with increase in ramp angle following the initial pressure rise. Fig. 7 shows the wall shear stress distribution for the different ramp angles studied. For the weakest interaction, a sharp drop in the wall shear stress is observed close to the corner location leading to a small negative value. Negative shear stress signifies negative velocity gradients associated with the reversed (negative) velocity in the separation bubble. This negative shear stress strengthens the observation of separation in the 8° ramp configuration studied. The separation length of the interaction is very small which can be concluded from the zeros of the function indicating the separation and reattachment point. With increasing shock strength, the length to which the adverse pressure gradient is propagated upstream increases. The magnitude of the negative shear stress also increases as seen in Fig. 7.



**Fig. 6:** Comparison of surface pressure distributions for 8° - 24° ramps at  $M = 2.85$



**Fig. 7:** Wall Shear Stress Distribution for 8° - 24° ramps at  $M = 2.94$ .

#### 4. Conclusion

Flow has been simulated for compression ramps of deflection angles ranging from 8-24° at Mach numbers 2.85 and 2.95. The numerical results have been compared with experimental results and analysed. Using the density contours and shear stress plots, incipient separation was observed at 16°, and a fully separated situation has been observed explicitly showing the separation and reattachment shocks for higher deflection angles. The surface pressure distributions predicted by the CFD Code for the 2-D compression ramps based on SST of k- $\omega$  and Realizable k- $\epsilon$  turbulence models have shown greater tendency to separate, due to an effect of the low Reynolds number employed in the models. The SST k- $\omega$  turbulence model has predicted the separation region earlier.

Moderate to significant discrepancies occur in the strong and very strong interactions. The data curves for the computed and experimental pressure ratios (20°, and 24°), of strong interactions, show over prediction at separation and under prediction at reattachment locations. The stronger the interaction, the more the numerical solutions deviates from experimental results since, the turbulence model itself is not accurately modeling the flow physics of the problem for stronger interactions. This is the limitation of the turbulence model.

#### 5. Acknowledgment

The author is sincerely thankful to Ministry of Defence, and Defence University, College of Engineering, Debrezeit, Ethiopia, for supporting and sponsoring this work.

#### References

- [1] Arnal, D., and Delery, J. M., "Laminar-Turbulent Transition and Shock-Wave/Boundary- Layer Interaction," RTO-EN-AVT-116, Chapter 4, 2004, pp. 1-46, May 2004.
- [2] Oliver et al: "Assessment of Turbulent Shock-Boundary Layer Interaction Computations Using the OVERFLOW Code," School of Aeronautics and Astronautics Purdue University, January 2007.
- [3] Asmelash Haftu and Amarjit Singh: "Numerical Analysis of Shock Wave Turbulent Boundary Layer Interaction over a 2-D Compression Ramp," *International Journal of Advanced Engineering sciences and Technologies (IJAEST)*, Vol No. 5, Issue No. 2, 144-149, April 2011.
- [4] Asmelash Haftu et al: "Numerical simulation of ramp induced shock wave boundary layer interaction in turbulent flow," *The Royal Aeronautical Journal*, Volume 177, No 1192, UK, June 2012.
- [5] G Jagadeesh, Fascinating World of Shock Waves, August 2008.

